Crystalline Coordination Polymers of Flavonoid with Zinc: Preparation, Solid State Structure, and Functional Properties

Qiuyu Zhang[a], Hongling Zheng[a], Siyu Chen[a], Dejian Huang*[,ab]

a. Department of Food Science & Technology, National University of Singapore, 2 Science Drive 2, Singapore 117542, Singapore.

b. National University of Singapore (Suzhou) Research Institute, 377 Linquan Street, Suzhou, Jiangsu, 215123, China.

Contents

1. Experimental Section

1.1 General

All chemicals were of analytical grade and used without further purification unless otherwise stated. Zinc acetate dihydrate ($Zn(CH_3CO_2)_2.2H_2O$) and D-(+)-glucose solution were obtained from Merck & Co., Inc. Flavonoid diosmetin, kaempferol, fisetin, quercetin and luteolin were purchased from BLD Pharmatech Ltd, Shanghai, China. Tryptic soy broth (TSA; Oxoid, Co.), N,N-dimethylformamide (DMF) and methanol (MeOH) and ethanol (EtOH) were purchased from Thermo Fisher Scientific Co., Ltd. 96 Well TC-treated microplates were purchased from Corning Inc. 10X Phosphate-buffered saline (PBS) were purchased from Vivantis Technologies Sdn. Bhd. All aqueous solutions were prepared with 18.2 MΩ·cm ultrapure water obtained from Millipore water purification system.

1.2 Synthetic procedures

Synthesis of zinc-flavonoid crystalline network (Zinc-quercetin, Zinc-fisetin, Zinc-diosmetin). The solvothermal method was used for the synthesis of zinc-flavonoid crystalline networks. Flavonoids (e,g., quercetin, fisetin, diosmetin) (0.34 mmol) was dissolved in 2 mL of EtOH in a 4 mL glass vial. NaOH (1.0 M) was added to the reaction mixture (75 µL for quercetin and fisetin, 50 µL for diosmetin), followed by addition of solid $Zn(CH_3CO_2)_2.2H_2O$ (150 mg, 0.68 mmol). The reaction mixture was sonicated and placed in oven 60 ^oC for 4 days. The resulting solids were collected by filtration to remove the reaction solvent and excess reactants, washed with EtOH and water, and air-dried to yield 118 mg Q-Zn (69%), 96 mg F-Zn (53%), and 126 mg D-Zn (77%).

Synthesis of zinc-luteolin crystalline network. Luteolin (100.18 mg, 0.35 mmol) were dissolved in 2.25 mL of MeOH in a 4 mL glass vial. 250 µL NaOH (1.0 M) was added to the reaction mixture, followed by the addition of solid $Zn(CH_3CO_2)_2.2H_2O$ (155 mg, 0.70 mmol). The reaction mixture was sonicated and placed in an 80 ^oC oven for 4 days. The resulting solid was collected by filtration, washed with MeOH and water to remove residual reagents, and air-dried to give 124 mg product (68.0%).

Activation of the Zinc-flavonoid crystalline networks

The obtained zinc-flavonoid crystalline polymers were soaked in either EtOH or MeOH for 1 day, and the solvent was replaced for 3 consecutive days. On day 4, the mixtures were filtered, and the residues were dried under vacuum to obtain the activated crystalline polymers.

1.3 Characterization methods

UV-Vis spectra were measured on a Biotek Epoch 2 Microplate Spectrophotometer equipped with BioTek Gen5 version 3.02 software or Shimazu UV-1600 equipped with UVProbe 2.70 software. The flavonoids were dissolved in DMSO/EtOH and the absorbance of 270-550 nm wavelength range were scanned. For the quantification of the amounts of flavonoids in the crystalline materials, the polymers were suspended in EtOH and dissociated by the addition of 1M HCl. The solutions were transferred to 96 well plate and the absorbances at different wavelength were recorded for different flavonoids ($\lambda_{fistein}$ = 364 nm, $\lambda_{kaempferol}$ = 367 nm, $\lambda_{quercetin}$ = 374 nm, $\lambda_{luteolin}$ = 351 nm and $\lambda_{diosmetin}$ = 344 nm). The flavonoid monomers were dissolved in EtOH in concentrations ranging from 0.1 to 1.0 mM for the standard curve calibration.

Powdered X-ray Diffraction (PXRD) spectra were measured using a Rigaku SmartLab X-ray diffractometer with Cu Kα radiation (40 kV, 40 mA) at room temperature, with a 2θ scan range of 3° to 50°. Fourier Transform Infrared (FTIR) spectra were recorded in the range of 4000 – 400 cm^{-1} using a Perkin Elmer Spectrum Two spectrometer. Thermogravimetric Analysis (TGA) was carried out under a nitrogen (N_2) atmosphere using a TA instrument Q500, with a heating rate of 10 °C/min from 40 to 800 °C. The morphologies of the crystalline materials were examined using a FEI QUANTA 650 FEG scanning electron microscopy SEM after sputter-coating the solid powder of activated polymers with gold. Inductively coupled plasma optical emission spectroscopy (ICP-OES) was used to quantify zinc ions present in the crystalline polymer using a Perkin Elmer Avio 500 ICP-OES. Prior to the analysis, the solid samples were digested using HNO_3/HCl (3:1) in a microwave at 240 °C for 15 min and topped up to 15 mL with deionized water. The C and H contents of samples were determined using a modified Dumas combustion method. Samples were weighed into tin containers and combusted at high temperature in the presence of excess oxygen. The resulting combustion gases are carried by helium flow through a GC column attached to a thermal conductivity detector (TCD). Nitrogen adsorption–desorption isotherms of the activated polymers were measured at 77 K using Quantachrome Instruments Autosorb-iQ2. Brunauer–Emmett–Teller (BET) Surface areas and total pore volume were calculated from the N_2 isotherm. The non-local

density functional theory (NL-DFT) model in Quantachrom ASiQwin 5.0 software package was used to calculate the pore size distribution. Solid-state ^{13}C nuclear magnetic resonance (ssNMR) was conducted using a Bruker AVNEO400 solid-state NMR spectroscopy (400 MHz, wide bore, 4 mm probe). ^{1}H and ^{13}C NMR spectra were recorded on Bruker 500 MHz spectrometers. TopSpin 4.0.5 was used for NMR data collection and MestReNova v12.0.0 was used for NMR data analysis. Chemical shifts are reported in ppm from the solvent resonance as the internal standard: ^{1}H (DMSO-d_6: δ 2.50 ppm), ^{13}C (DMSO-d_6: δ 39.52 ppm). Data are reported as follows: chemical shift (δ ppm), integration, multiplicity (s = singlet, d = doublet, t = triplet, q = quartet, m = multiplet), and coupling constants (Hz).

2. Additional spectra and data

Table S1. Ligand and zinc contents of crystalline zinc–flavonoid coordination polymers determined by UV-Vis spectroscopy and ICP-OES.

	%(w/w) Ligand (from UV-Vis)	**%(w/w) Zn (from ICP)**	**Molar ratio (L:Zn)**
Q-Zn	50.41	20.94	1 : 1.92
L-Zn	47.52	23.06	1 : 2.12
D-Zn	69.18	17.37	1 : 1.15
F-Zn	40.53	24.51	1 : 2.65

Table S2. Elemental analysis results for crystalline zinc–flavonoid polymers determined by CHNS combustion analysis (C and H) and ICP–OES (Zn). Values are reported as weight percentages relative to the total sample mass.

	%(w/w) C	**%(w/w) H**	**%(w/w) Zn**
Q-Zn	38.89	2.55	20.94
L-Zn	39.18	2.81	23.06
D-Zn	48.35	3.28	17.37
F-Zn	37.46	2.59	24.51

Table S3. Frequencies of characteristic absorption bands in FT-IR spectra of kaempferol and Zn-Kae complex in cm^{-1}

Compound	*v* (C=O)	*v* (C=C)	*v* (C-O-C)	*v* (O-Zn)
Quercetin	1661	1519	1165	-
Q-Zn	1648	1495	1267	657
Fisetin	1615	1568	1248	-
F-Zn	1622	1488	1266	617
Diosmetin	1650	1499	1139	-
D-Zn	1632	1531	1257	622
Luteolin	1651	1504	1165	-
L-Zn	1627	1482	1225	616

Table S4. Pore volume of crystalline polymers

	Q-Zn	**F-Zn**	**L-Zn**	**D-Zn**
Pore volume	0.044 cc/g	0.148 cc/g	0.223 cc/g	0.054 cc/g

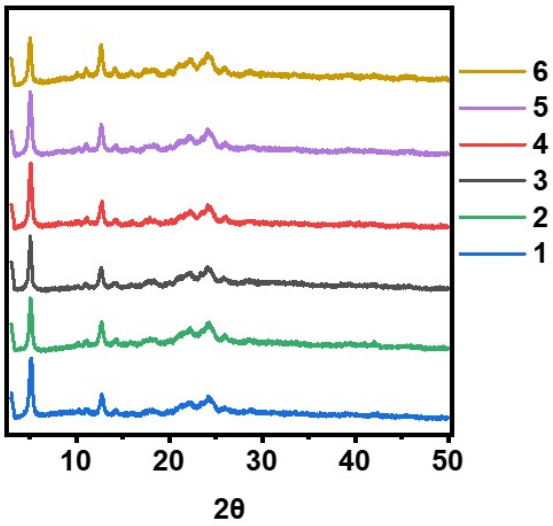

Figure S1. PXRD patterns of six independently synthesized batches of Q-Zn, showing consistent diffraction features and comparable crystallinity across different preparations, supporting the reproducibility of the synthetic protocol.

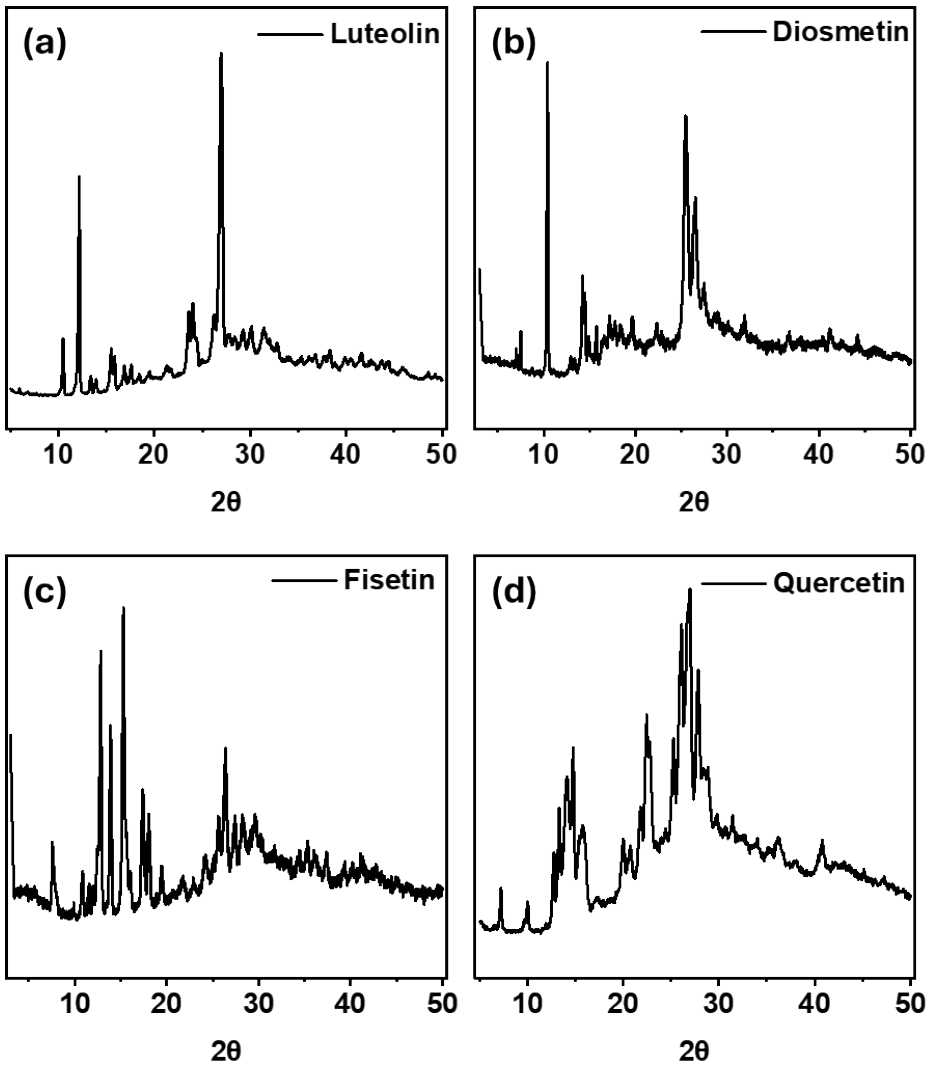

Figure S2. Powder XRD patterns of (a) Luteolin, (b) Diosmetin, (c) Fisetin and (d) Quercetin.

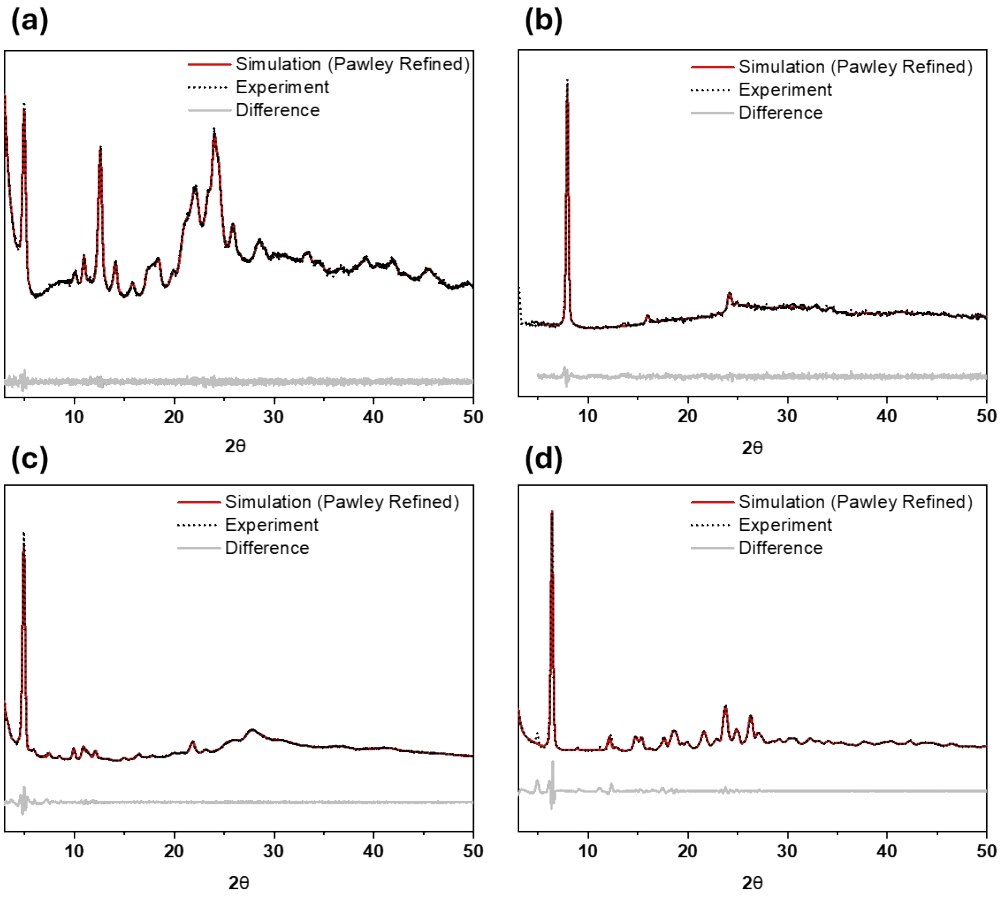

Figure S3. Comparison of experimental (black points) and calculated (red line) patterns of(A) zinc-quercetin polymer (Q-Zn), (B) zinc-luteolin polymer (L-Zn), (C) zinc-fisetin polymer (F-Zn), (D) zinc-diosmetin polymer (D-Zn), confirming the purity of the solid. Laboratory X-ray powder diffraction data were collected on a Rigaku SmartLab X-ray diffractometer with CuKα radiation at room temperature, with a 2θ scan range of 3° to 50°.

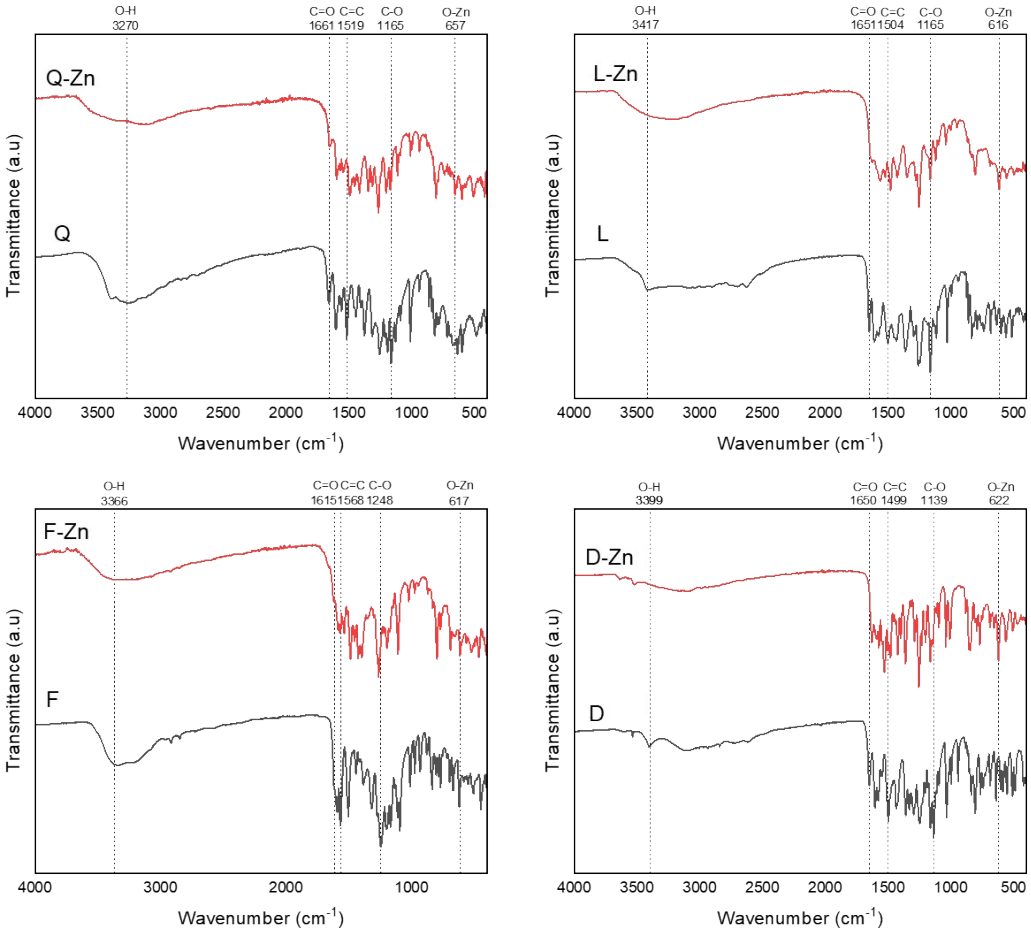

Figure S4. FTIR spectra of the flavonoid monomers (Q, L, F, D) and their corresponding zinc coordination polymers (Q-Zn, L-Zn, F-Zn, D-Zn). Key spectral shifts in the carbonyl and hydroxyl regions confirm coordination between Zn^{2+} ions and flavonoid ligands, supporting successful framework formation.

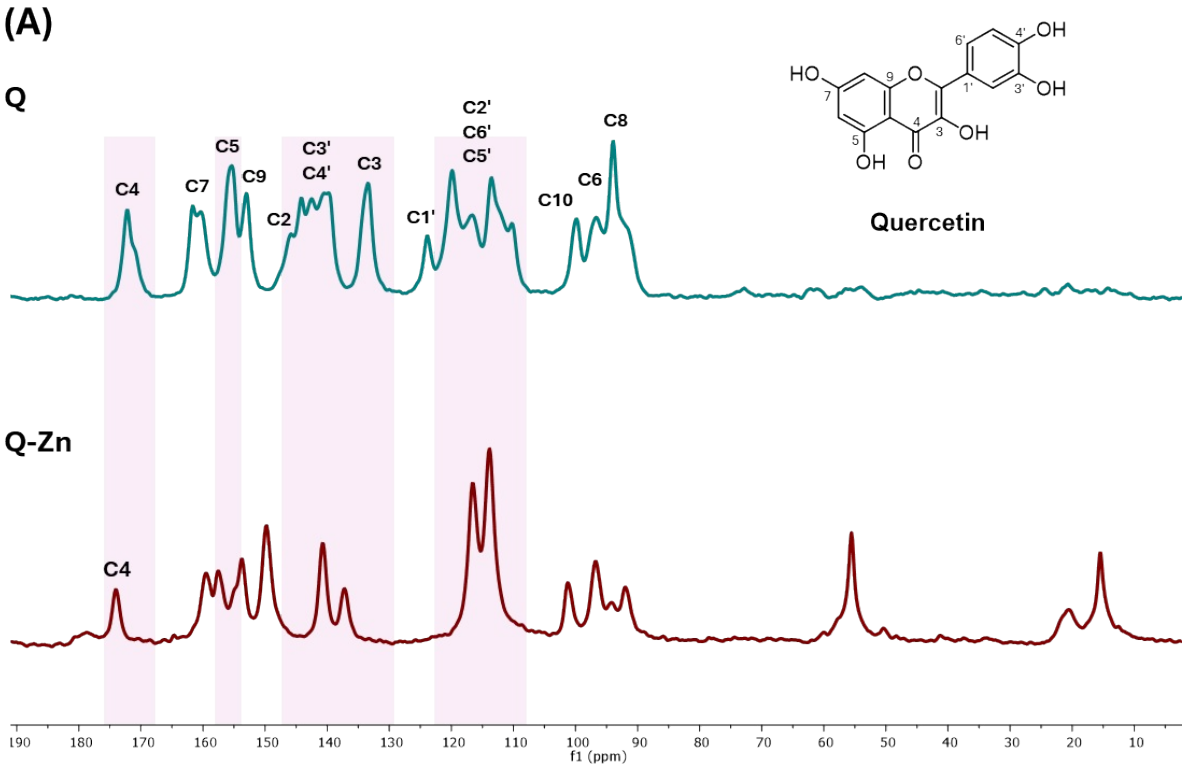
(A)
Q
C4
C7
C5
C9
C2
C3'
C4'
C3
C1'
C2'
C6'
C5'
C10
C6
C8
Quercetin
Q-Zn
C4
190 180 170 160 150 140 130 120 110 100 90 80 70 60 50 40 30 20 10
f1 (ppm)

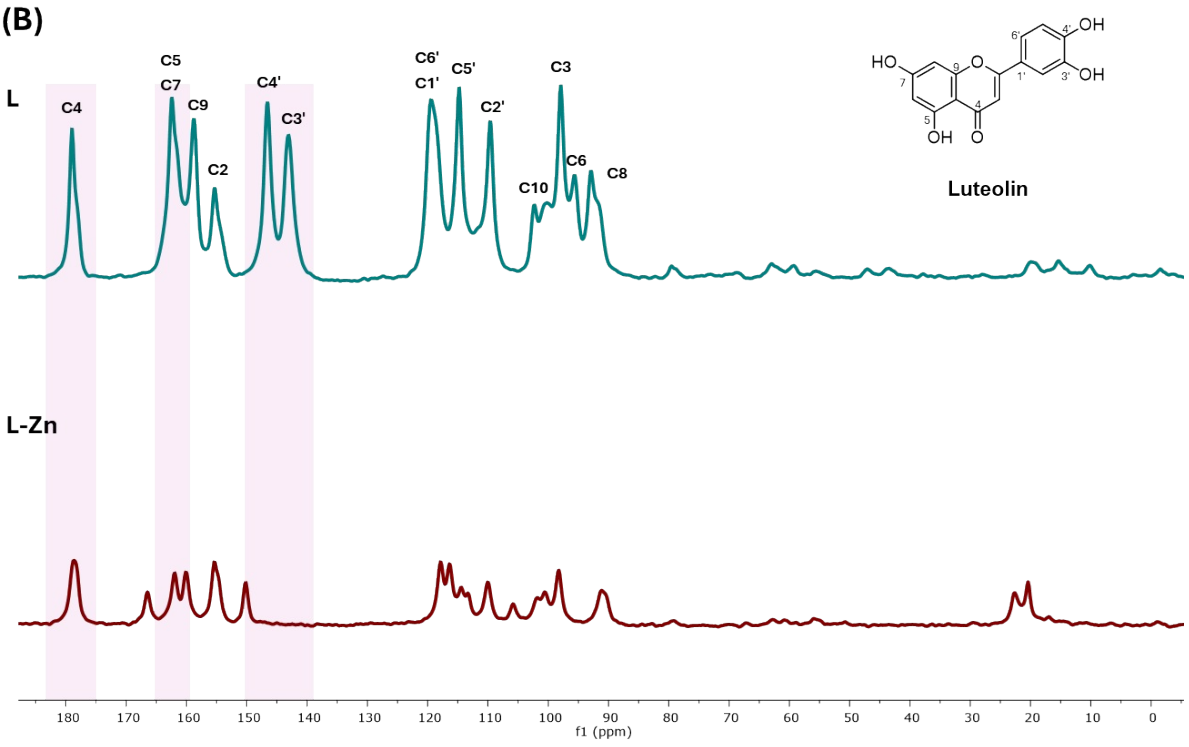
(B)
L
C4
C5
C7
C9
C2
C4'
C3'
C6'
C1'
C5'
C2'
C3
C10
C6
C8
Luteolin
L-Zn
180 170 160 150 140 130 120 110 100 90 80 70 60 50 40 30 20 10 0
f1 (ppm)

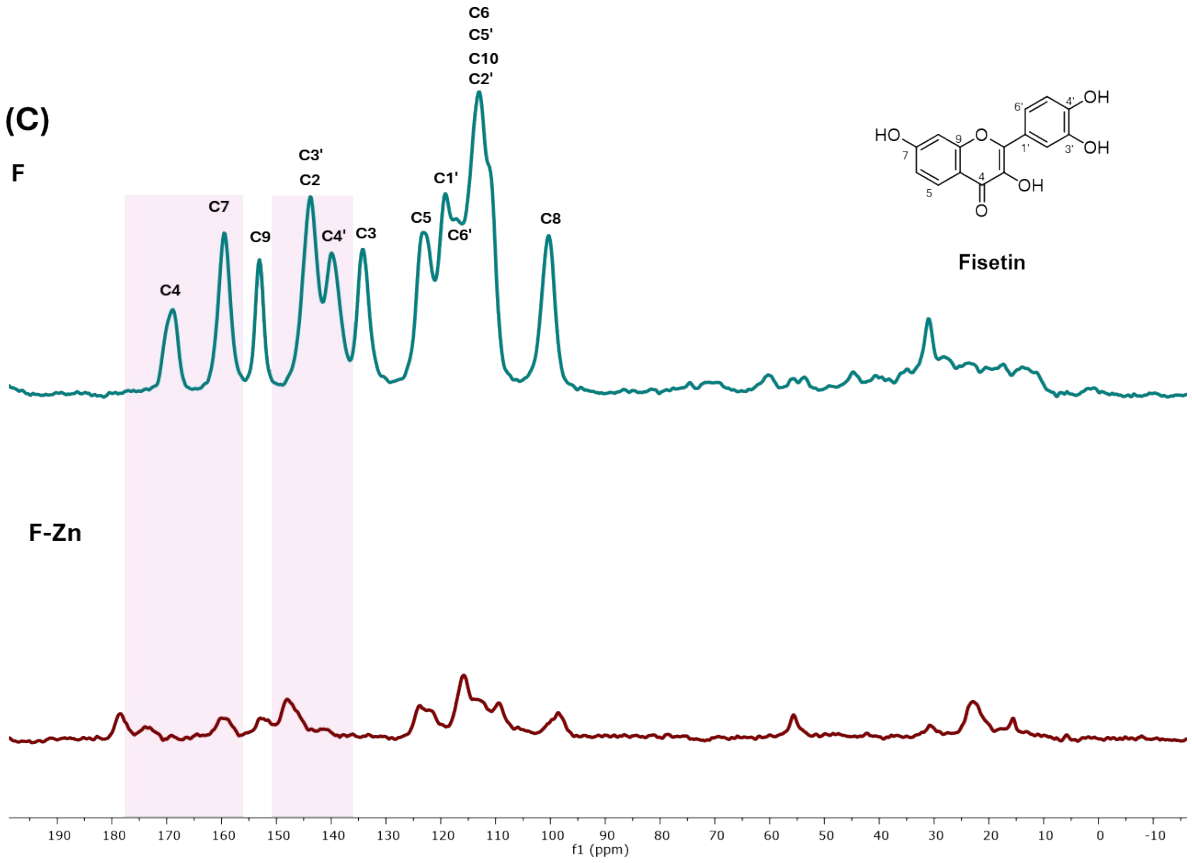
(C)
F
C6
C5'
C10
C2'
C3'
C2
C1'
C7
C9
C4'
C3
C5
C6'
C8
C4
HO
OH
OH
OH
Fisetin
F-Zn
190 180 170 160 150 140 130 120 110 100 90 80 70 60 50 40 30 20 10 0 -10
f1 (ppm)

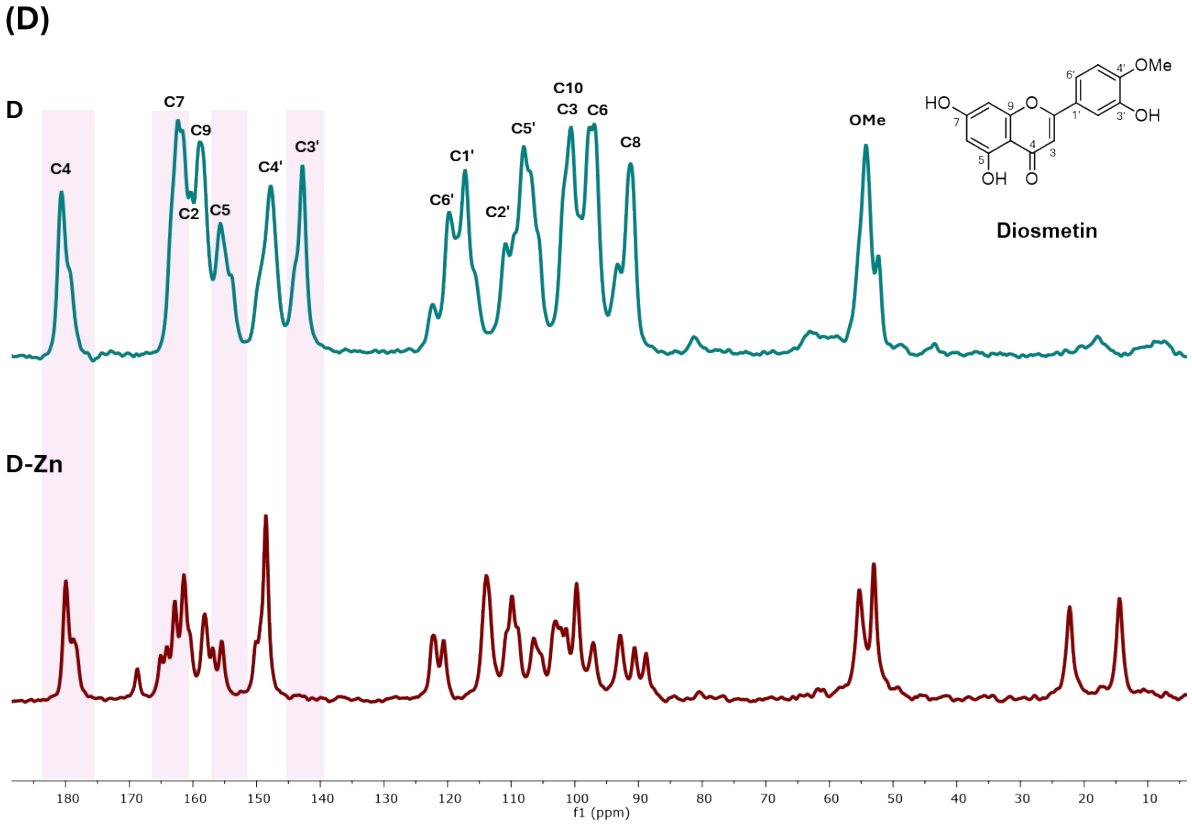
(D)
D
C7
C9
C4
C2
C5
C4'
C3'
C1'
C6'
C2'
C5'
C10
C3
C6
C8
OMe
HO
OMe
OH
OH
Diosmetin
D-Zn
180 170 160 150 140 130 120 110 100 90 80 70 60 50 40 30 20 10
f1 (ppm)

Figure S5. ^{13}C solid state NMR of flavonoid and crystalline polymer. (**A**) quercetin and Q-Zn. (**B**) luteolin and L-Zn. (**C**) fisetin and F-Zn (**D**) Diosmetin and D-Zn

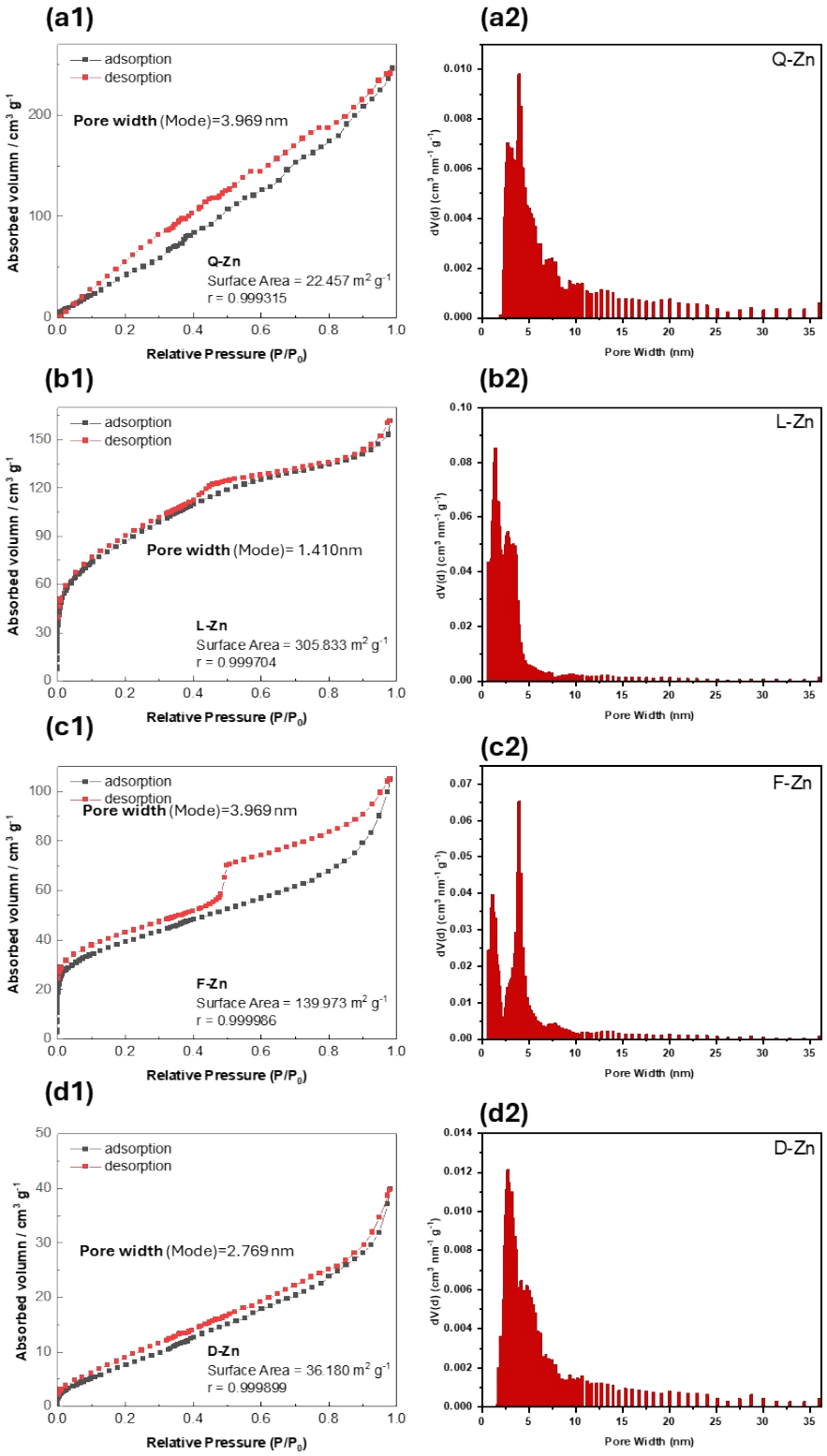

Figure S6. N_2 adsorption–desorption isotherms of (a1) **Q-Zn**, (b1) **L-Zn**, (c1) **F-Zn** and (d1) **D-Zn** with their mode pore width and pore size distribution of (a2) **Q-Zn**, (b2) **L-Zn**, (c2) **F-Zn** and (d2) **D-Zn** obtained by NLDFT method.

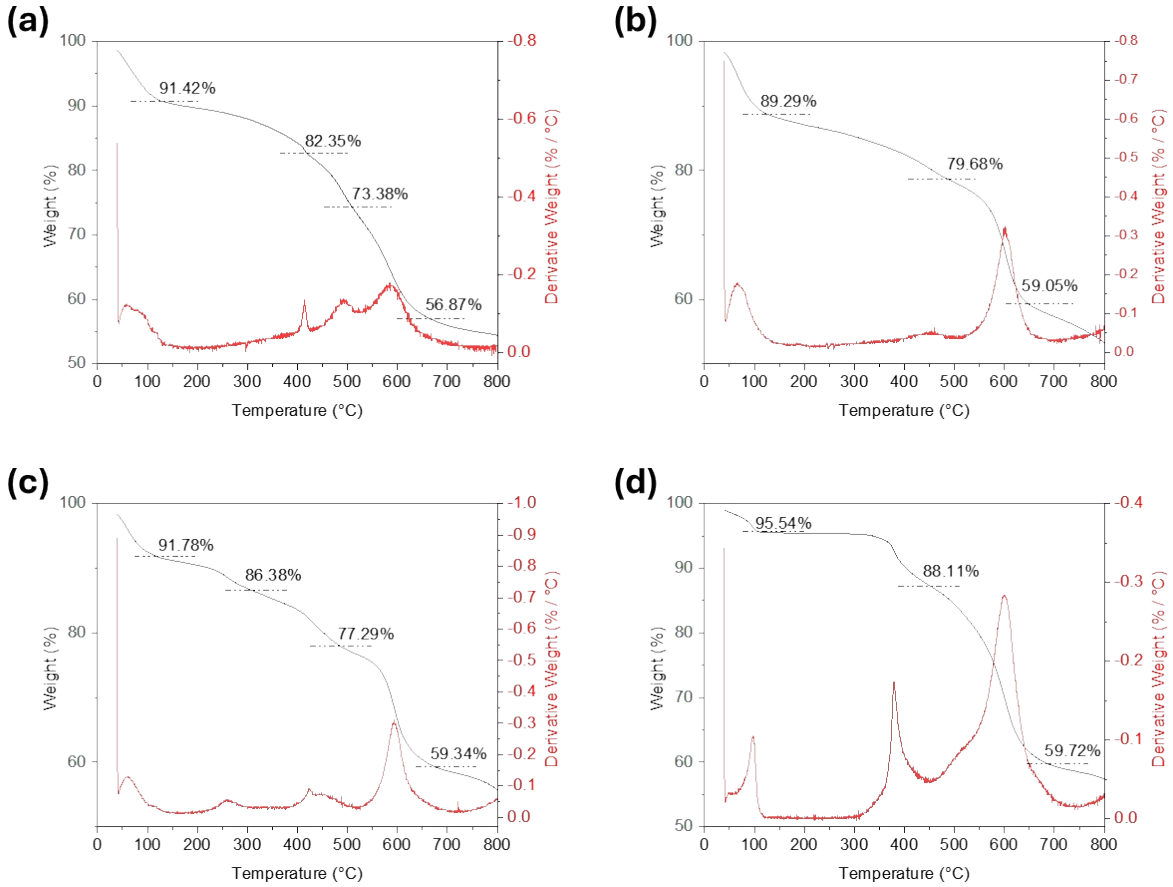

Figure S7. TGA of crystalline polymer (**a**) Q-Zn, (**b**) L-Zn, (**c**) F-Zn and (**d**) D-Zn

3. Supplementary note 1: Ligand and Metal Quantification

3.1 Degradation of Crystalline Polymers and Ligand Recovery

To confirm the reversibility of the coordination frameworks and verify that the flavonoid ligands remain structurally intact after polymer formation, degradation experiments were first carried out[1]. Four representative crystalline materials—F-Zn, Q-Zn, D-Zn and L-Zn—were each subjected to acidic breakdown. Approximately 10 mg of each sample was dispersed in 1.5 mL of absolute ethanol, followed by the addition of 100 μL of 1 M HCl. Upon acid addition, the initially heterogeneous suspensions gradually transformed into clear solutions, indicating effective disassembly of the coordination frameworks. The resulting solutions were then passed

rapidly through short silica columns to remove zinc salts, and the eluted organic fractions were dried under vacuum. The recovered solids were redissolved in DMSO-d_6 and analyzed by ^{1}H NMR spectroscopy.

The aromatic regions of the recovered ligands were in excellent agreement with those of the corresponding starting materials, confirming structural fidelity. Minor differences observed in the OH proton region were attributed to solvent effects and proton exchange dynamics under acidic conditions. These results demonstrate that the ligand structures remain chemically unchanged upon release from the coordination network and validate the use of degradation-based methods for subsequent quantification studies. Representative recovery results, including visual changes during dissolution and NMR comparisons, are provided in **Figure S8**.

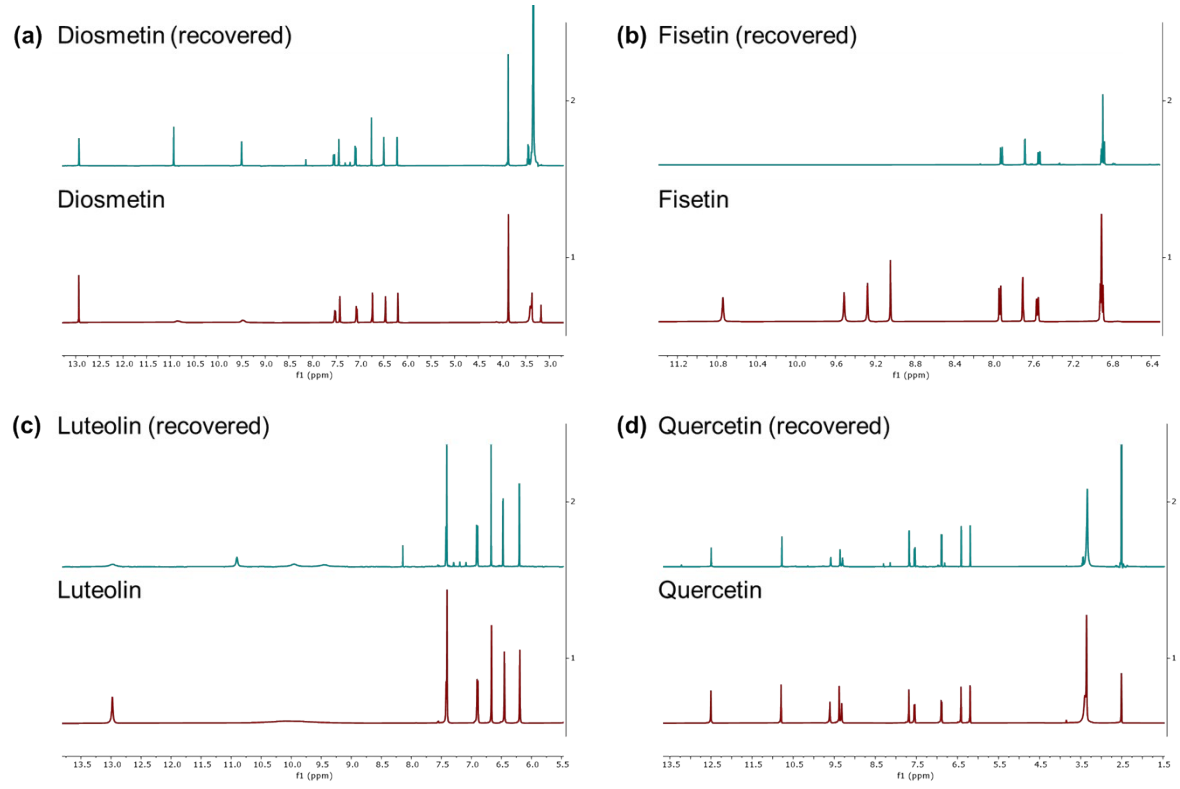

Figure S8. Comparison of ^{1}H NMR spectra of recovered flavonoid ligands (top, blue) and their corresponding pure standards (bottom, red) for (a) Diosmetin, (b) Fisetin, (c) Luteolin, and (d) Quercetin. (400M, DMSO-d_6, 298K)

3.2 Quantification of ligands and metal

Following structural verification of the recovered ligands, quantification of both organic and inorganic components was carried out to determine the ligand-to-metal stoichiometry of the crystalline polymers. For ligand analysis, samples were first digested by dispersing the solid in

ethanol, followed by the addition of 1 M HCl to facilitate full decomposition. After 1 hour of digestion at room temperature, the resulting clear solutions were transferred to a 96-well plate and analyzed using a microplate reader. To determine the concentration of released flavonoid ligands, calibration curves were done for each monomer using the same setup. Prior to calibration, UV–Vis absorption spectra of the individual flavonoids in ethanol were recorded to identify their maximum absorption wavelengths (λ_{max}), which ranged from 344 to 374 nm depending on the compound (**Figure S9**). Standard solutions were prepared from 1 mM stock solutions by serial dilution to obtain final concentrations of 0, 10, 25, 50, 100, and 250 µM. The absorbance at λ_{max} was measured in a 96-well plate, and calibration curves were obtained by linear fitting of absorbance versus concentration **(Figure S10**). These curves were then used to quantify the ligand content in the digested samples.

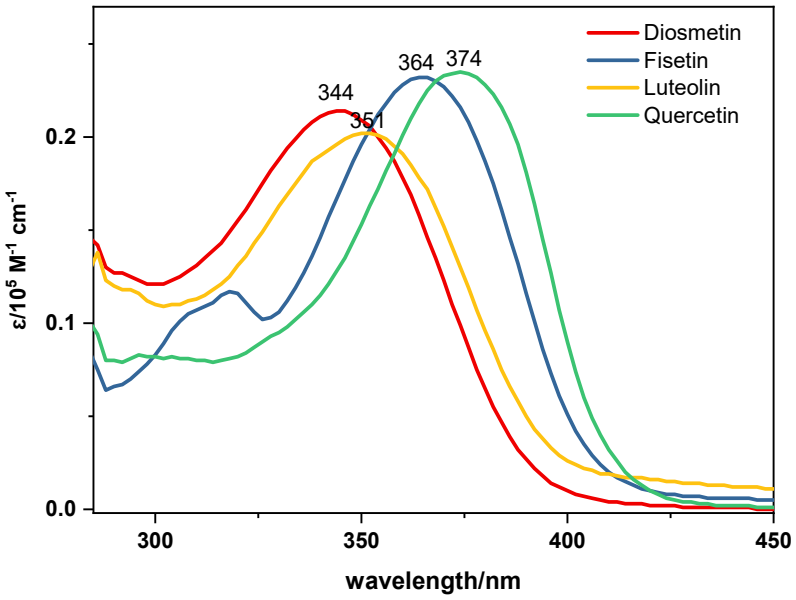

Figure S9. UV–Vis absorption spectra of four flavonoid ligands: diosmetin, fisetin, luteolin, and quercetin in ethanol.

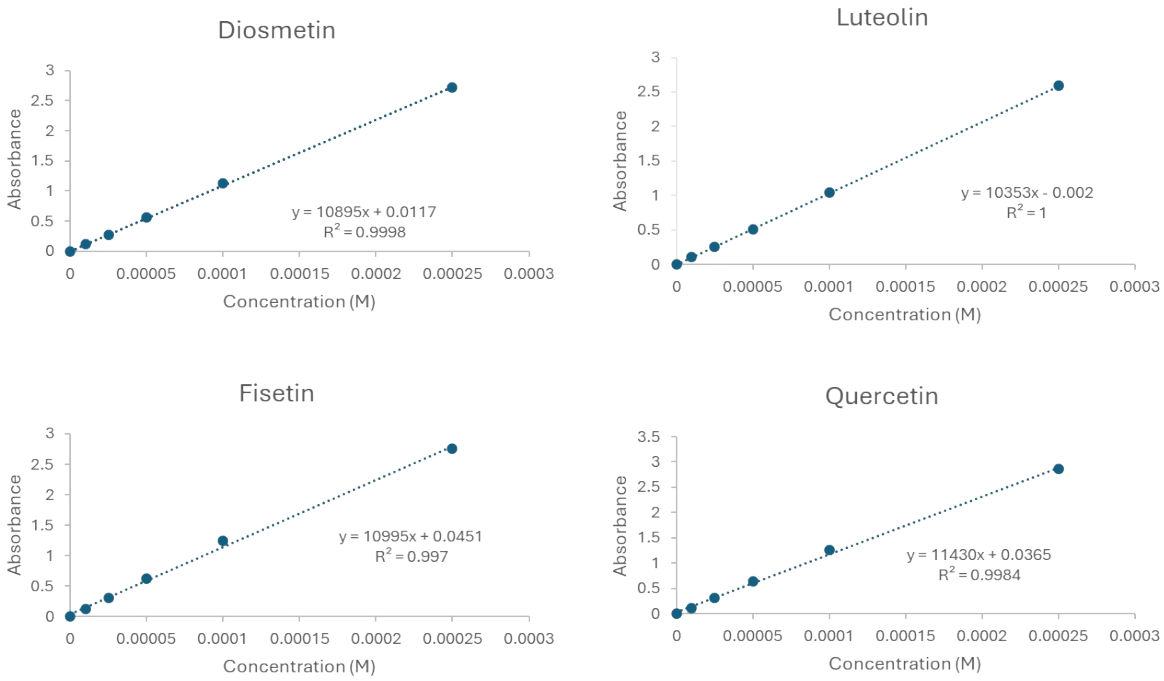

Figure S10. Calibration curves for diosmetin, luteolin, fisetin, and quercetin in ethanol.

Zinc quantification was performed using inductively coupled plasma–optical emission spectrometry (ICP-OES). Samples were digested using a 3:1 mixture of HNO_3 and HCl in a closed-vessel microwave digestion system at 240 °C for 15 minutes. The digests were subsequently diluted to a final volume of 15 mL with ultrapure water prior to analysis.

The resulting weight percentages of ligand and zinc, along with calculated ligand-to-metal molar ratios, are summarized in the **Table S1**. Among the polymers, F-Zn exhibited the highest metal content, corresponding to a molar ratio of approximately 1:3 (L:Zn), while D-Zn had the highest ligand content and the lowest Zn loading, with a ratio close to 1:1.2. These variations reflect the different coordination capacities of the flavonoid ligands and suggest that structural and electronic factors influence their metal-binding stoichiometry.

4. Supplementary note 2: Aqueous Stability

To evaluate the aqueous stability of the flavonoid-based crystalline polymers, samples(50mg) were dispersed in 5 mL of aqueous solution at pH 1, 3.5, neutral water (pH ~7), and pH 9, and incubated at room temperature for 24 hours. After soaking, 5 mL of DMSO was added to each sample to ensure complete solubilization of any leached flavonoid ligands. The mixtures were then centrifuged to remove residual solids, and the resulting supernatants were analyzed using a microplate reader. Quantification of the released ligands was performed using calibration

curves prepared in 1:1 (v/v) H_2O:DMSO mixtures. For each flavonoid, a stock solution of 10^{-3} M was serially diluted to generate a calibration curve: 1×10^{-5}, 2.5×10^{-5}, 5×10^{-5}, 1×10^{-4}, 2.5×10^{-4}, and 5×10^{-4} M. Absorbance was measured at 360 nm for all samples (**Figure S11**).

PXRD measurements were conducted on the residual solids obtained after 24-hour soaking in solutions of pH 3.5, 7.0, and 9.0 to assess the impact of aqueous environments on crystallinity.

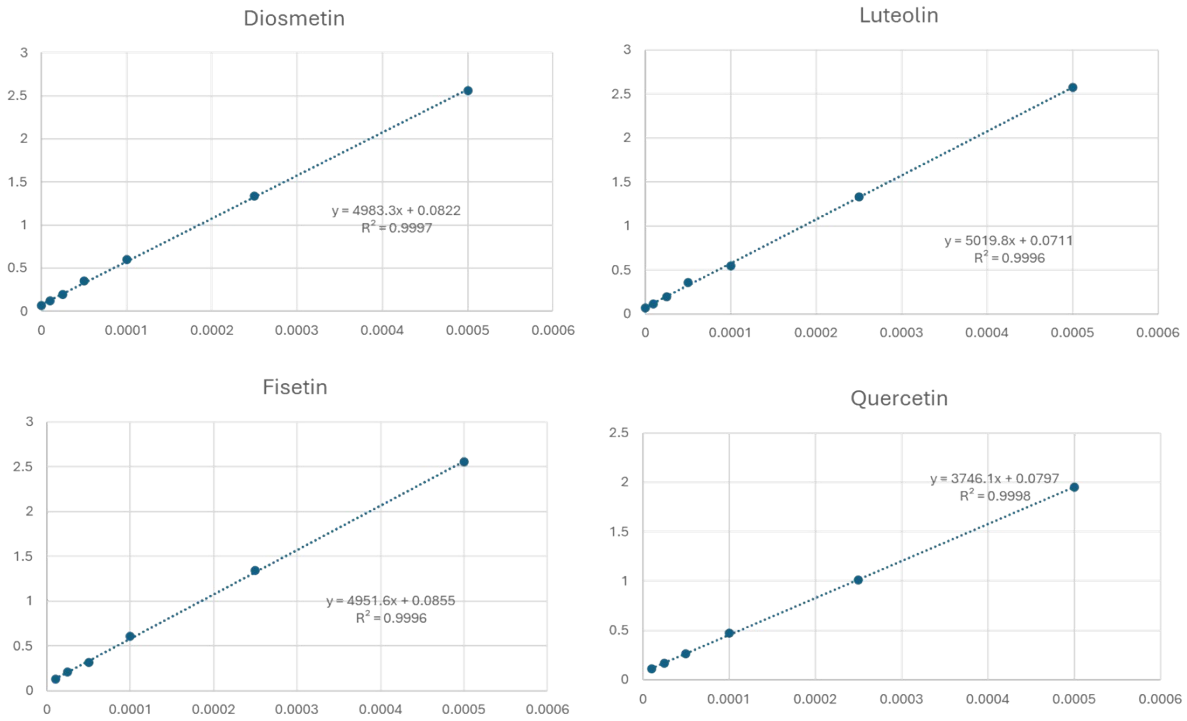

Figure S11. Calibration curves for diosmetin, luteolin, fisetin, and quercetin in 1:1 (v/v) H_2O:DMSO.

Table S5. The ligand concentrations in μM for each crystalline polymer sample after 24-hour soaking at pH 3.5, neutral water, and pH 9.

	pH=3.5	**Ultra pure water**	**pH=9.0**
D-Zn	645.52	465.31	387.86
L-Zn	134.05	102.57	55.36
F-Zn	29.99	23.73	25.55
Q-Zn	9.69	9.16	8.89

5. Supplementary note 3: Bacteria Biofilm Inhibition Assay

The bacteria biofilm inhibition potential of the synthesized materials was assessed using the crystal violet staining method against *Staphylococcus aureus* ATCC BAA-1768 (MRSA), following the procedure reported by Haney and coworkers with slight modifications[2]. Briefly, frozen bacteria were revived by inoculating them in TSB and incubating at 37 °C with shaking at 180 rpm. The overnight culture was diluted 1:100 into fresh TSB and grown to mid-log phase (OD_{600} = 0.4). Mid-log phase bacterial cultures were diluted 1:200 in fresh TSB supplemented with 1% glucose.

Stock solutions of quercetin, diosmetin, fisetin, luteolin, $Zn(OAc)_2 \cdot 2H_2O$, Q–Zn, D–Zn, F–Zn, and L–Zn were prepared in DMSO at a concentration of 12.8 mg mL^{-1}. For crystalline polymers, the suspensions were ultrasonicated for 30 min prior to use to ensure uniform dispersion.

As shown in **Figure S12**, 800 µL of diluted bacterial suspension were added to the wells highlighted in blue. Subsequently, 16 µL of each stock solution were added to wells A1 and C1 (highlighted in green), followed by addition of 784 µL of diluted bacterial suspension to afford a final concentration of 128 µg mL^{-1}. 800 µL of samples from each green well were serially transferred to the next column and thoroughly mixed to generate a twofold dilution series (from A1 to B2 and C1 to D2). Controls were prepared by combining diluted bacterial suspension with DMSO (negative control), while blank wells contained only broth. The plates were incubated at 37 °C for 48 h.

	1	2	3	4	5	6
A/S1	128	64	32	16	8	4
B/S1	2	1	control	control	control	Blank
C/S2	128	64	32	16	8	4
D/S2	2	1	control	control	control	Blank

Figure S12. Sample arrangement in a 24 well plate

After incubation, the spent growth media were carefully discarded by inverting the plates, and the wells were rinsed once with distilled water. The plates were inverted and air-dried completely on sterile paper towels. Each well was then treated with 1 mL MeOH, incubated for 20 min, and gently inverted to remove the solvent. The plates were dried at 60 °C. The adhered biomass was stained with 900 µL of 0.1% (wt/vol) crystal violet (CV) solution and

incubated at 37 °C for 30 min. The CV solution was removed, and the wells were washed gently with PBS solution. Plates were again dried at 60 °C to ensure complete solvent removal. The bound CV was solubilized using 1 mL of 30% (v/v) acetic acid and shaken gently to ensure homogeneity. The absorbance was recorded at 595 nm using a Cytation 5 Cell Imaging & Multimode Plate Reader. The percentage inhibition was calculated using the equation below:

$$\%\ inhibtion = \frac{ABS_{control} - (ABS_{sample} - ABS_{blank})}{ABS_{control}}$$

Subsequently, the data were used to find the IC_{50} of the biofilm inhibition using non-linear regression on GraphPad Prism 9 software.

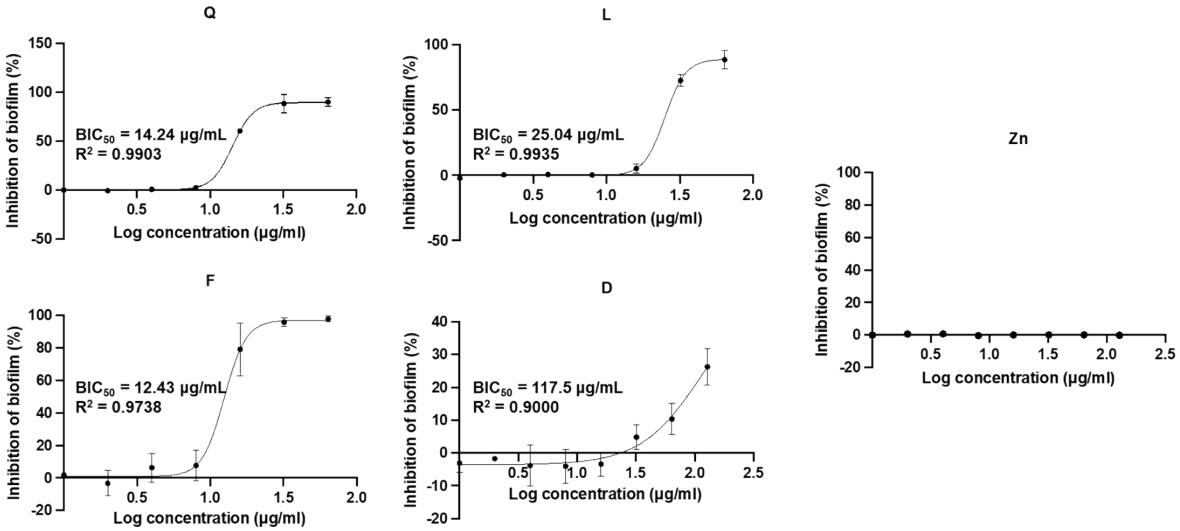

Figure S13. Graphs of % inhibition of biofilm against log concentration for quercetin, diosmetin, fisetin, luteolin and $Zn(OAc)_2 \cdot 2H_2O$. BIC_{50} values are annotated.

6. References

(1) Han, S.; Lah, M. S. Simple and Efficient Regeneration of MOF-5 and HKUST-1 via Acid–Base Treatment. *Cryst. Growth Des.* **2015**, *15* (11), 5568–5572. https://doi.org/10.1021/acs.cgd.5b01218.

(2) Haney, E. F.; Trimble, M. J.; Hancock, R. E. W. Microtiter Plate Assays to Assess Antibiofilm Activity against Bacteria. *Nat. Protoc.* **2021**, *16* (5), 2615–2632. https://doi.org/10.1038/s41596-021-00515-3.